END
DATE
FILMED
5 83
DTIC

MICROCOPY RESOLUTION TEST CHART
NATIONAL BUREAU OF STANDARDS-1963-A

AFWAL-TR-82-3095

CALIBRATION OF C-130 LIGHTNING CHARACTERIZATION
SENSORS

W. P. Geren
Mechanical/Electrical Systems Technology Organization
Boeing Military Airplane Company
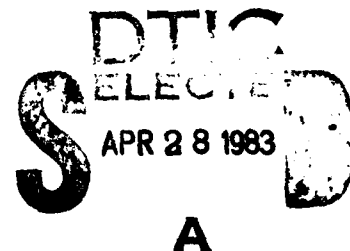Seattle, Washington 98124

December 1982

Final Report for Period July 1981 - September 1982

APPROVED FOR PUBLIC RELEASE DISTRIBUTION UNLIMITED

FLIGHT DYNAMICS LABORATORY
AIR FORCE WRIGHT AERONAUTICAL LABORATORIES
AIR FORCE SYSTEMS COMMAND
WRIGHT-PATTERSON AIR FORCE BASE, OHIO 45433

DTIC
ELECT
APR 2 8 1983

A

83 04 27 028

BRIAN P. KUHLMAN, LT.
PROJECT ENGINEER

GARY A. DUBRO, CHIEF
ATMOSPHERIC ELECTRICITY HAZARDS GROUP
FLIGHT VEHICLE PROTECTION BRANCH
VEHICLE EQUIPMENT DIVISION

FOR THE COMMANDER

SOLOMON R. METRES
DIRECTOR
VEHICLE EQUIPMENT DIVISION

REPORT DOCUMENTATION PAGE		READ INSTRUCTIONS BEFORE COMPLETING FORM
1. REPORT NUMBER AFWAL-TR-82-3095	2. GOVT ACCESSION NO. AD-A127	3. RECIPIENT'S CATALOG NUMBER 344
4. TITLE (and Subtitle) CALIBRATION OF C-130 LIGHTNING CHARACTERIZATION SENSORS		5. TYPE OF REPORT & PERIOD COVERED Final Technical Report 1 July 1981 - 30 Sept. 1982
		6. PERFORMING ORG. REPORT NUMBER
7. AUTHOR(s) W. P. Geren		8. CONTRACT OR GRANT NUMBER(s) Contract: F33615-81-C-3409
9. PERFORMING ORGANIZATION NAME AND ADDRESS Mechanical/Electrical Systems Technology Organiza- tion Boeing Military Airplane Company Seattle, Washington 98124		10. PROGRAM ELEMENT, PROJECT, TASK AREA & WORK UNIT NUMBERS 24020235
11. CONTROLLING OFFICE NAME AND ADDRESS Flight Dynamics Laboratory AF Wright Aeronautical Laboratory, AFSC Wright-Patterson AFB, OHIO 45433		12. REPORT DATE December 1982
		13. NUMBER OF PAGES 45
14. MONITORING AGENCY NAME & ADDRESS(if different from Controlling Office)		15. SECURITY CLASS. (of this report) Unclassified
		15a. DECLASSIFICATION/DOWNGRADING SCHEDULE

16. DISTRIBUTION STATEMENT (of this Report)

Approved for public release; distribution unlimited.

17. DISTRIBUTION STATEMENT (of the abstract entered in Block 20, if different from Report)

18. SUPPLEMENTARY NOTES

19. KEY WORDS (Continue on reverse side if necessary and identify by block number)

Lightning electromagnetic fields
Analytical Modelling
Lightning Sensors
In-flight data

Antenna analysis
Transfer functions
Data reduction
Airframe resonances
Peak rate-of-rise

20. ABSTRACT (Continue on reverse side if necessary and identify by block number)

An analytical model for calculating transfer functions relating the C-130
lightning sensor responses to incident electromagnetic fields was developed.
The model consists of two components; a low frequency non-resonant term and a
frequency-dependent term including airframe resonances. The latter are
calculated for the frequency range 1-10 MHz and compared with measured data.
Recommendations for removing airframe resonances from the measured data are
presented.

DD FORM 1473 1 JAN 73   EDITION OF 1 NOV 65 IS OBSOLETE

FOREWORD

This final technical report was submitted by the Mechanical/Electrical Systems
Technology Research Organization of the Advanced Airplane Branch of the Boeing
Military Airplane Company in September 1982 under Contract F33615-81-C-3409.
The effort entitled, "Calibration of C-130 Lightning Characterization
Sensors," was sponsored by the Flight Dynamics Laboratory, Air Force Wright
Aeronautical Laboratories, Wright-Patterson Air Force Base, Ohio, with 2Lt.
Brian Kuhlman, AFWAL/FIESL, as the Project Engineer. W. P. Geren was the
Program Manager and Principal Investigator technically responsible for the
work, as well as the author of the report.

iii

TABLE OF CONTENTS

SECTION I

INTRODUCTION

This report describes an analytical model for the calculation of total
electric and magnetic fields induced on the surface of an aircraft by an
incident plane wave field. Transfer functions are presented for nine
lightning sensors in the form of equations for the non-resonant component.
For three sensors, transfer functions are computed over the 1-10 MHZ range and
compared with data.

1. BACKGROUND

Data on the radiated electromagnetic fields produced by lightning strikes
was gathered during the summers of 1981-82 in a joint National Oceanographic
and Atmospheric Administration (NOAA) and AFWAL/FIESL project. A WC-130
aircraft was equipped with electrically small antennas (lightning sensors) to
measure surface fields on the airframe.

As part of this program, the Boeing Company was contracted to provide
technical assistance in the calibration of the lightning sensors by
calculating transfer functions relating surface fields on the airframe to an
incident plane wave field.

2. OBJECTIVES

The overall objective of the effort described in this report was to
provide guidelines and quantitative methods for processing the C-130 lightning
sensor data. These methods are based upon the results of the analytical model
and will be used to remove the response of the airframe from the sensor data,
resulting in estimates of the incident electromagnetic fields. Specifically
the objectives were to:

    a. Develop an analytical model for calculating electromagnetic
        fields on the airframe surface.

    b. Calculate transfer functions for all lightning sensors.

c. Use the lightning sensor data from the 1981-82 flight program, along with the corresponding transfer functions, to infer quantitative methods for removing airframe effects from the data.

SECTION II
TECHNICAL APPROACH

Currents induced on the surface of a relatively thick structure, such as an aircraft fuselage, may be decomposed into three components:

a.   Axial currents with no azimuth variations (resonant).

b.   Axial currents with azimuthal variation (non-resonant).

c.   Azimuthal currents (non-resonant).

As described in reference 1, currents of type a. may be obtained from a thin wire model of the airframe. The corresponding surface current density is obtained by dividing the total current by the effective circumference. Surface currents of type b. or c. may be approximated in the low frequency limit (i.e., wavelength>>effective radius), by expressions for scattering from cylinders (fuselage) and strips (wings). These expressions are simple and require minimal computation. The thin wire model, however, requires the solution of an integral equation. The two model types will be referred to throughout as "non-resonant" and "resonant", since all airframe resonance effects are contained in the thin wire model.

One method for solving thin-wire problems is the method of moments. In the method of moments, the airframe structure is subdivided into equivalent wire segments. Coupling between the segments is calculated, resulting in an impedance matrix which is then used to relate induced currents to incident fields. This technique is well established but requires large computers and elaborate input data. We opted in this program for the approach described in reference 2. In this alternate method, the integral equation is solved by obtaining approximate analytical solutions. In the lowest (zeroth) order approximation, the current on each airframe member i.e., forward fuselage, right wing, left wing, aft fuselage, vertical stabilizer, right horizontal stabilizer, and left horizontal stabilizer, is expressed as the sum of a sinusoidal term, with undetermined coefficients, and a forced term, proportional to the tangential electric field. Imposing current and charge

3

conservation at the intersections, along with the boundary condition that the
current goes to zero at wing tips, fuselage nose, and stabilizer tips,
determines the sinusoid coefficients. The first order correction is obtained
by the iteration procedure described in reference 3. The thin-wire model
developed under this contract includes the first order correction and is in
good agreement with results published by R. W. P. King. The results shown in
Figs. 1 and 2 for symmetric and antisymmetric currents induced in an equi-arm
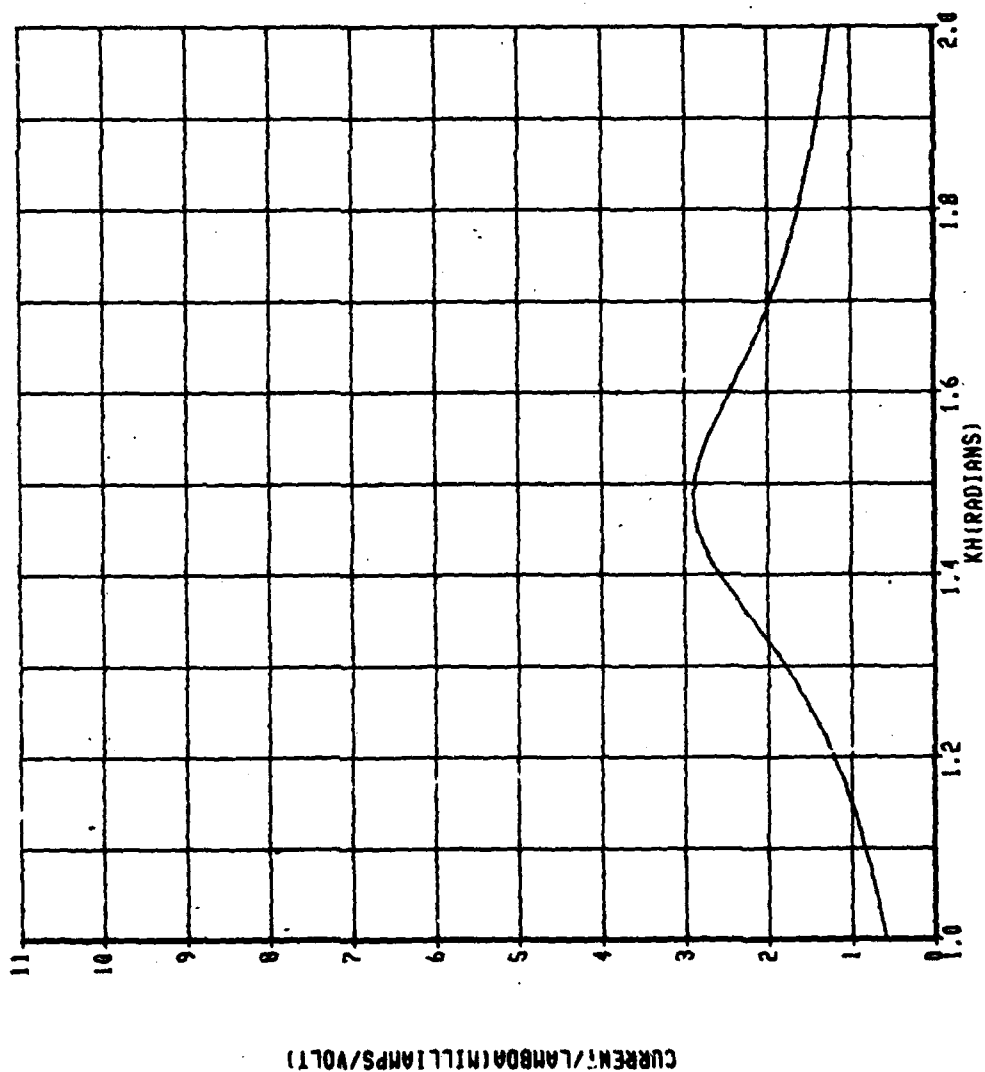cross are to be compared with Ref. 3, Fig. 3.

Figure 1   Symmetric current at center of equi-arm cross calculated from thin-wire model for comparison with published results (see text).

5

ALPHA,THETA,PHI=
0.000000   45.000000   90.000000
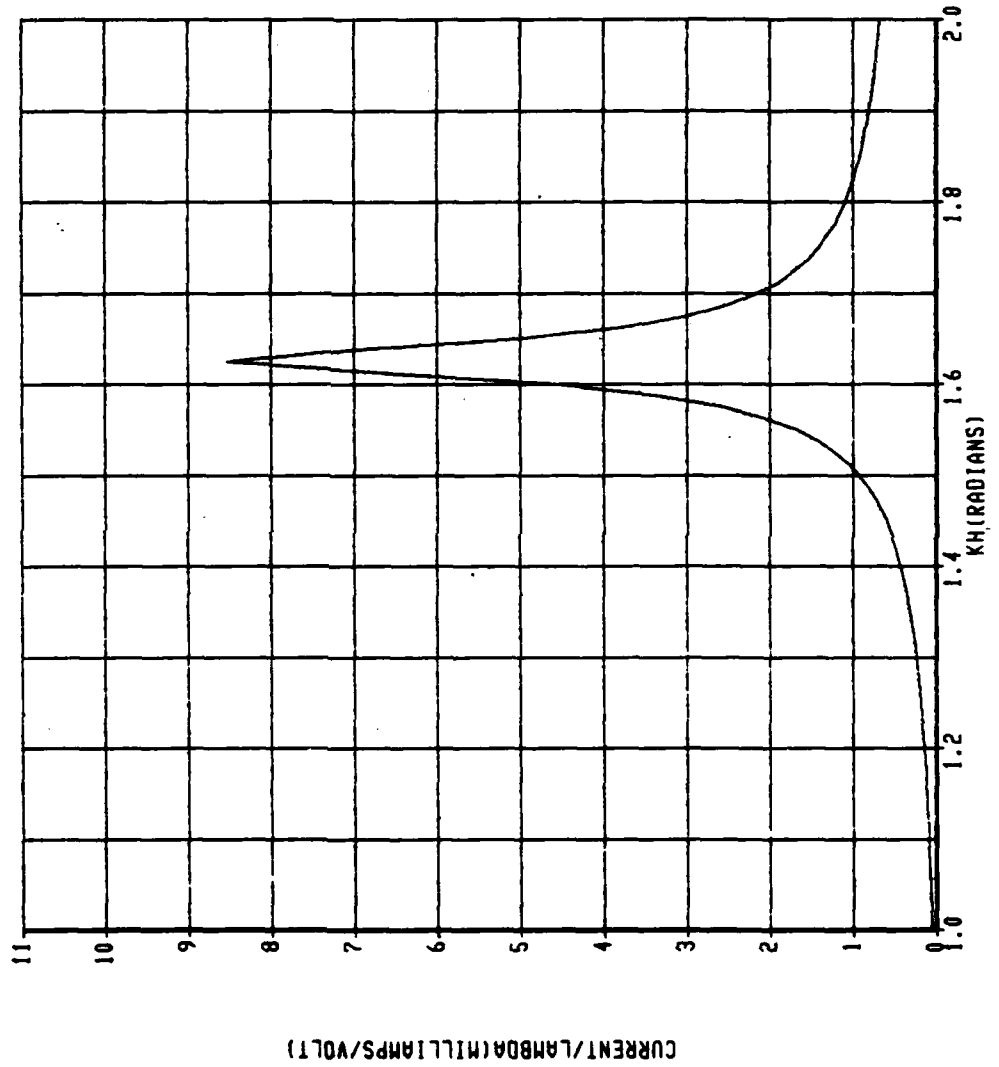
KH(RADIANS)

CURRENT/LAMBDA(MILLIAMPS/VOLT)

Figure 2   Anti-symmetric current at center of equi-arm cross calculated from thin-wire model for comparison with published results (see text).

SECTION III

DESCRIPTION OF ANALYTICAL MODEL

As described previously, the surface currents may be obtained from two independent models, one which gives the net current on each airframe member, and another which gives azimuthally-varying and azimuthally-directed currents. The total surface current at a given location is the vector sum of the two. The surface charge density, q, is obtained from the conservation law:

$$\text{div}\vec{J} + jwq = 0$$

where $\vec{J}$ is the surface current density, div is the divergence operator, and w is the radial frequency.

Choose the aircraft coordinates as follows (see Figure 3):

x-axis	directed forward along fuselage
y-axis	directed along the left wing
z-axis	upward

and the lightning channel coordinates as follows:

$\bar{x}$-axis	parallel to y-axis
$\bar{y}$-axis	anti-parallel to x-axis
$\bar{z}$-axis	parallel to z-axis
• origin at location of ground strike	

Rho, theta, phi are the spherical coordinates of the aircraft in the $(\bar{x},\bar{y},\bar{z})$, or lightning channel reference system.

1. THIN WIRE MODEL

The thin wire model provides the net current and charge on the airframe at a given location. The corresponding surface current and charge are obtained by dividing by the effective circumference. For the fuselage, which is cylindrical, the effective circumference is the geometrical circumference.
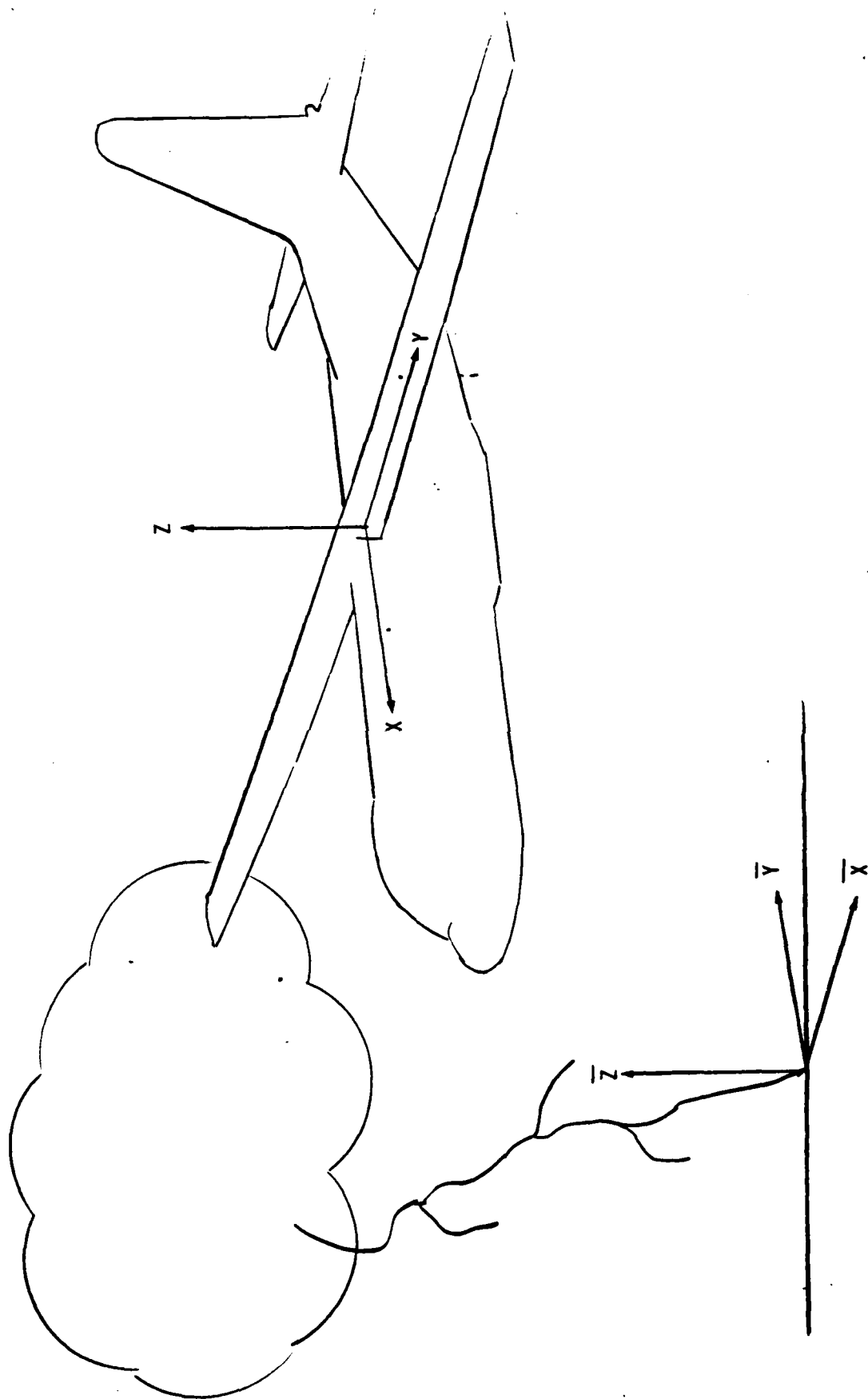
Figure 3   Coordinate systems.

8

For the the wings, the effective circumference is the geometrical circumference, multiplied by a concentration factor which varies from typically .5 in mid-chord to 4 or 5 near an edge.

2. CYLINDER AND PROLATE SPHERICAL MODELS (FUSELAGE)

Using the approach described in reference 1, the surface current density induced on a cylinder with axis along the x-axis is given by:

$$\vec{J} = (\vec{J}_A + 2\ \hat{\theta}\cdot\vec{H}_{inc})\hat{x} - \hat{x}\vec{H}_{inc}\ [1 - 2j\hat{k}\cdot\vec{r}]\hat{\theta}$$

where: $\vec{H}_{inc}$ = incident magnetic field

$\vec{J}_A$ = total axial current/circumference

$\hat{\theta}$ = $-\sin\theta\ \hat{y} + \cos\theta\ \hat{z}$

$\vec{r}$ = $a(\cos\theta\hat{y} + \sin\theta\hat{z})$

$\hat{k}$ = wave number

a = radius of cylinder

The normal electric field is obtained from the conservation of charge and is given by:

$$E_n = E_{nA} + 2\hat{n}\cdot\vec{E}_{inc}$$

where: $\vec{E}_{inc}$ = incident electric field

E_{nA} = $q_A/EPSO$, q_A = $(j/kc)dJ_A/dx$

c = velocity of light

$EPSO$ = permittivity of free space

9

For E-field antennas located near the extremeties of the fuselage, the prolate spheroid model is of use. The normal electric field induced on the surface of a prolate spheroid of major and minor axis a and b, respectively, is given, in the quasistatic approximation, by (major axis along x-axis):

$$E_n = F_x E_{xinc}(x/a) + F_r E_{rinc}(r/a)$$

where: $(x/a)^2 + (r/b)^2 = 1$

$$\hat{r} = \cos\theta \, \hat{y} + \sin\theta \, \hat{z}$$

$F_x, F_r =$ functions of eccentricity, e

$$e = (1 - (b/a)^2)^{.5}$$

Note that the quasistatic prolate spheroid model includes coupling to the axial component of $\vec{E}_{inc}$ which is the low frequency limit of the resonant model.

3. STRIP MODEL (WING)

The surface currents induced on the upper surface of the wing are obtained from the thin wire model and the infinite strip (see reference 4) and are given by the expression:

$$J_y = J_A + H_{xinc} - K_W H_{zinc}$$

where: $J_A =$ total axial current/effective circumference

$H_{inc} =$ incident magentic field

$K_W = t/((W/2)^2 - t^2)^{.5}$

$W =$ wing width

$t =$ distance from mid-chord to sensor in the positive x-direction

SECTION IV
DESCRIPTION OF SENSOR TRANSFER FUNCTIONS

The nine lightning sensors are listed in Table I. As indicated in the table, the sensors measure the time derivatives of the surface electromagnetic fields. According to the vendor's data sheets, the sensor outputs into the specified load are proportional to the time derivative of the field at the sensor, and all have a bandwidth (3 dB point) in excess of 38 MHz. Hence, the transfer function relating sensor output to time derivative of surface field is a frequency-independent factor given in the vendor's data sheets. The remainder of the overall transfer function relating sensor output to incident field is given by the analytical model.

The location of the sensors determines the choice of effective circumference and, in some cases, the importance of the contribution of the thin wire model. The sensors are discussed individually in the following.

A. General Description of Analytical Models for Sensors

1. Sensors #1 through #3, #6 and #7

These sensors are all located on the upper centerline of the fuselage. The effective circumference for all is just the fuselage circumference. Both thin-wire and cylinder models are required.

2. Sensors #4 and #9

Sensors #4 and #9 are located just forward of mid-chord and have a concentration factor of approximately .7, obtained from calculating the distribution of fields about the wing. Both the thin wire model and the strip model are required for these sensors.

3. Sensor #5

This sensor presents a different sort of geometry, with the effective circumference dependent on the two principal radii of curvature of the wing

11

TABLE I - C-130 LIGHTNING CHARACTERIZATION SENSORS

Sensor	Model	Type	Use	Location	Name
1	EG&G FPD-2(A)	D-dot	Electric Field	Forward Upper Fuselage	E-FUF
2	EG&G CML-S7A(A)	B-dot	Wing Axis H-Field	Forward Upper Fuselage	J-NT
3	EG&G CML-S7A(R)	B-dot	Fuselage Axis H-Field	Forward Upper Fuselage	J-WW
4	EG&G CML-7(R)	B-dot	Wing Surface Current	Left Upper Wing	J-LUW
5	EG&G RPD-2B(R)	D-dot	Wing Electric Field	Left Wingtip	E-LWT
6	EG&G HSD-S1A(R)	O_s-dot	Electric Field	Aft Upper Fuselage	E-AUF
7	EG&G CML-S7A(R)	B-dot	Fuselage Surface Current	Aft Upper Fuselage	J-AUF
8	EG&G FPD-2(A)	D-dot	Electric Field	Aft Lower Fuselage	E-ALF
9	EG&G CML-7(R)	B-dot	Wing Surface Current	Right Upper Wing	J-RUW

12

tip. A reasonable first approximation is that the effective radius of curvature for charge density is the geometric mean of the two principal radii of curvature (in the plane of the wing and normal to the plane of the wing). Only the thin wire model is required for this sensor.

4. Sensor #8

This sensor is similar in its complexity to the wing tip sensor. The sensor is located at the junction of the horizontal stabilizer and fuselage, so that the total charge is the sum of the charges induced on the two. The effective circumference is obtained by considering how this net charge distributes over the junction area. Below the first resonance of the horizontal stabilizer, it will act as a capacitive load on the fuselage, and the charge will spread out approximately uniformly over the horizontal stabilizer. Both the thin wire and prolate spheroid models are required for this sensor.

B. Conventions for Units and Transfer Functions

In order to organize the transfer functions and data, all transfer functions will be divided into two types, E-field and H-field. The E-field transfer function is defined as the normal component of the E-field at the sensor location/incident E-field and is dimensionless. The H-field transfer function is the surface current density at the sensor location/incident H-field, and has two vector components. Since surface current density has the same units as H-field, the H-field transfer function is also dimensionless.

For the non-resonant models, the vector components of the incident field are expressed in the aircraft coordinate system (see Figure 3). For the resonant model, the incident field is the amplitude of the plane wave, which is described completely by the propagation vector and polarization angle. The equations for the non-resonant models are listed in Table II.

13

TABLE II - EQUATIONS FOR NON-RESONANT TRANSFER FUNCTIONS

1	E-FUF	$E_n = 2E_{zinc}$
2	J-NT	$J_x = 2H_{yinc}$
3	J-WW	$J_y = (1 - 2jk_z a)H_{xinc}$
4	J-LUW	$J_y = H_{xinc} - K_W H_{zinc}$
5	E-LWT	negligible
6	E-AUF	$E_n = 2E_{zinc}$
7	J-AUF	$J_z = -2H_{yinc}$
8	E-ALF	$E_n = -P_x E_{xinc} - P_z E_{zinc}$
9	J-RUW	$J_y = H_{xinc} - K_W H_{zinc}$

Note: P_x, P_z, K_W are described in Chapter 3 under the prolate spheroid and strip models. Estimated values are:

$$P_x = 5$$
$$P_z = 2$$
$$K_W = .4$$

SECTION V

RESULTS OF ANALYTICAL CALIBRATION AND COMPARISON WITH
DATA IN THE 1-10 MHZ RANGE

The equations for the non-resonant transfer functions of the analytical
model are shown in Table II and are self-explanatory. The thin-wire, or
resonant model is somewhat more complicated. The thin wire model has been
incorporated in a computer program which runs on the PDP 11/70. Results for
three sensor transfer functions, using the effective circumferences of Table
III, were obtained for an aircraft elevation angle 45°, relative to the
lightning coordinate system (see Figure 3), and a vertically polarized plane
wave (i.e. horizontal H-field) and the following azimuths:

1. Incidence along the nose.
2. Incidence at 45° to fuselage, between nose and left wing.
3. Incidence along the left wing.
4. Incidence along the tail.

The thin wire model may be used to obtain transfer functions for the
remaining sensors, as data becomes available. The JDOT-WW sensor was omitted
because its resonant response is negligible, as it couples primarily to the
non-resonant circumferential fuselage currents.

The complete set of C-130 resonances is quite complex (see Ref. 5, page
163). Excluding the effects of the HF wire, there are more than 10 airframe
resonances in the 3-10 MHZ range. There are no resonances below 3 MHZ. The
thin wire model was simplified by representing the aft fuselage by a single
cylinder, with an increased length to partially account for the empennage.
The justification for this is that the major resonances are determined by the
wing and gross fuselage structure. I.e., the addition of empennage details
will only add some fine structure and result in slight shifts of the major
resonances.

The three sensors which exhibited appreciable airframe resonance effects
and for which data were available are JNT-DOT (or B-DOT NT), JLUW-DOT (or
J-DOT LUW), and EALF-DOT (or D-DOT ALF). For each of the three, transfer

TABLE III - EFFECTIVE CIRCUMFERENCES FOR RESONANT MODEL

E-FUF	C_F	C_F = Fuselage Circumference
J-NT	"	
J-WW	"	
J-LUW	2W/.7	W = Wing Width
E-LWT	$(C_1 C_2)^{.5}$	$C_1 . C_2$ = Circumferences corresponding to the two principal radii of curvature of the wing tip
E-AUF	C_F	
J-AUF	C_F	
E-ALF$^+$	C_F	
J-RUW	2W/.7	

+ Complicated by junction of fuselage, horizontal and vertical stabilizers. C_F is an estimate.

functions were calculated and multiplied by an assumed lightning spectrum of $1/F^2$, to produce an estimate of the spectral response in the 1-10 MHZ range, and to show the relative magnitude of the various resonant peaks. The results are discussed in the following text.

o   JNT-DOT

The thin wire model predicts a pair of resonances at 3.5-4 MHZ and 4.2-4.8 MHZ with a null between (see Figures 4A-4D). The null is due to the aft fuselage-wing resonance and is described by R.W.P. King in Reference 3 (see Figure 4 and accompanying discussion on page 515 of Reference 3). There is a higher order resonance near 10 MHz. The pair of resonances, and the null location are quite sensitive to change in azimuth. Comparison with data (see Figures 7A-7C) shows general agreement with the lower resonances but no pronounced higher order resonance above 6 MHZ. Such resonances should occur (see Reference 1, Figure 18) for an aircraft of the C-130 geometry. Their absence indicates either a deficiency in the lightning spectrum at these frequencies (i.e., a faster than $1/F^2$ roll-off) or inadvertent filtering in the data acquisition and processing.

o   JLUW-DOT

The thin-wire model results (Figures 5A-5D) show a pair of resonances at 3.2-3.4 MHZ and 4.4-4.6 MHZ with an intervening null. The sensitivity to azimuth is quite apparent. Figure 8A has a pair of resonances at 3.4 and 4.8 MHZ which are probably related to those in Figures 5A-5D. Figure 8B shows a measured spectrum in which the 4.8 MHZ resonances dominates, and compares favorably with Figure 5A. Again, the data show no pronounced resonances above 6 MHZ, for the same reasons given previously.

o   EALF-DOT

The thin-wire results (see Figures 6A-6D) show a single resonance at 4.2-4.4 MHZ and, in three cases, a null centered at 2.5 MHZ with a marked increase up to the 1 MHZ value. This compares favorably with the measured data of Figures 9A and 9B. Figure 6C, in which there is no direct E-field

excitation of the fuselage, is in good qualitative agreement with the data of Figure 9C. Note that the resonance in the data occurs at 3.8 MHZ. The difference between this value and the 4.2-4.4 MHZ of the model is due in part to the absence of empennage detail in the model.
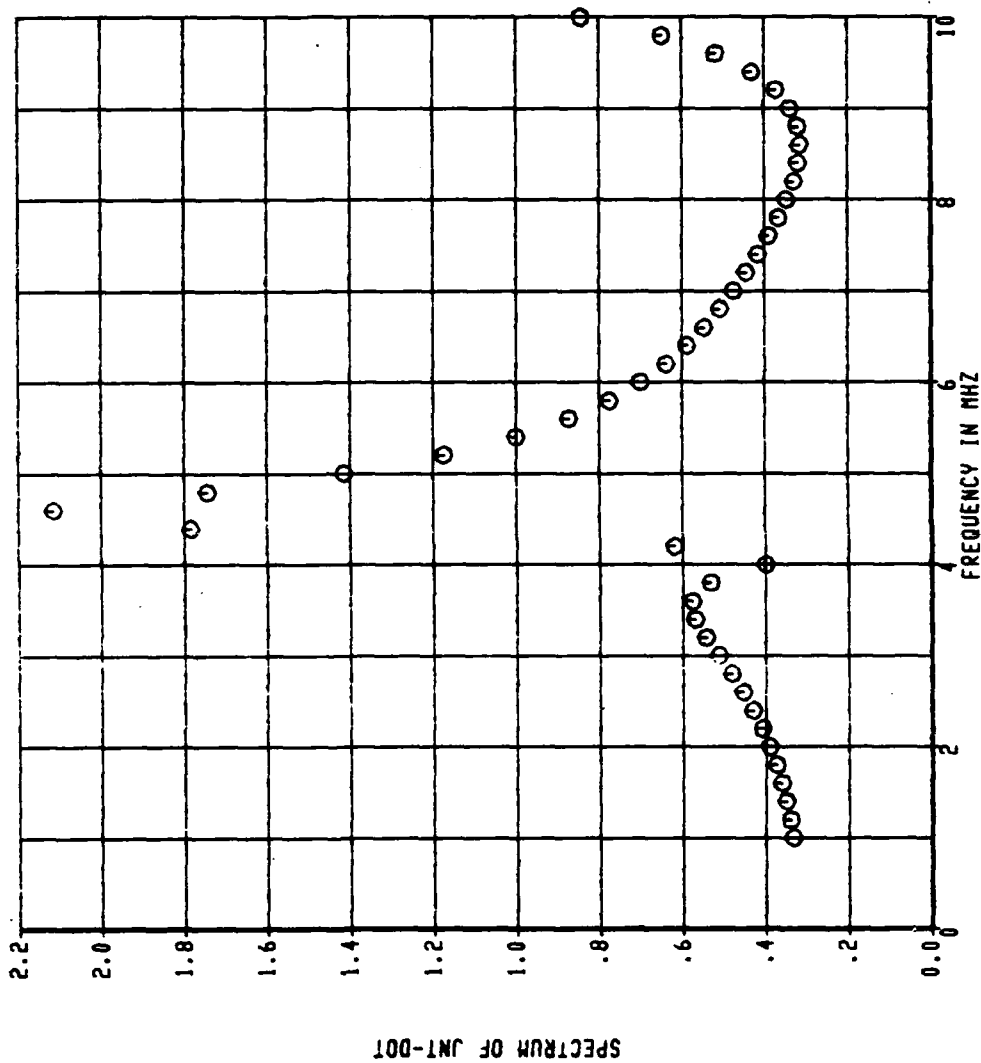
Figure 4A   Spectrum of JNT-DOT for incidence along nose obtained from thin-wire model.
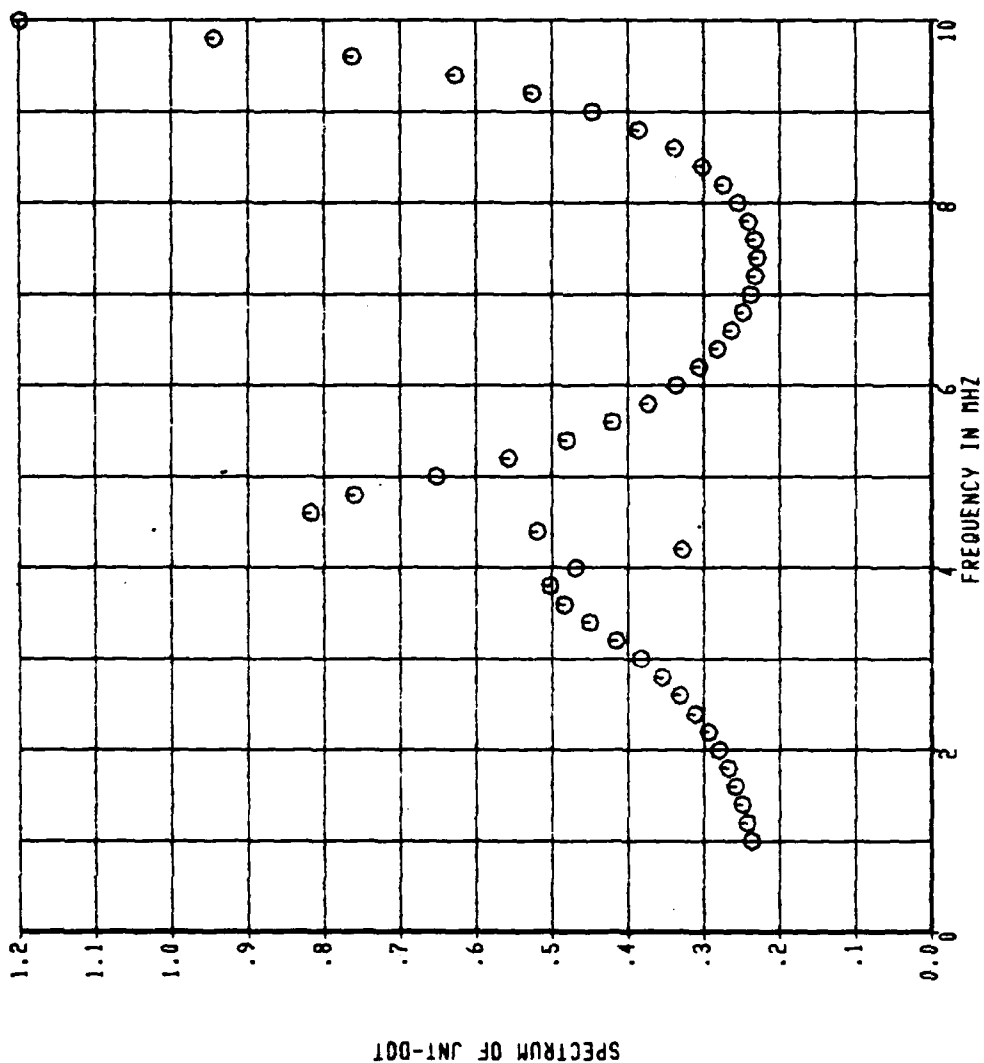
Figure 4B   Spectrum of JNT-DOT for incidence at 45° to fuselage obtained from thin-wire model.
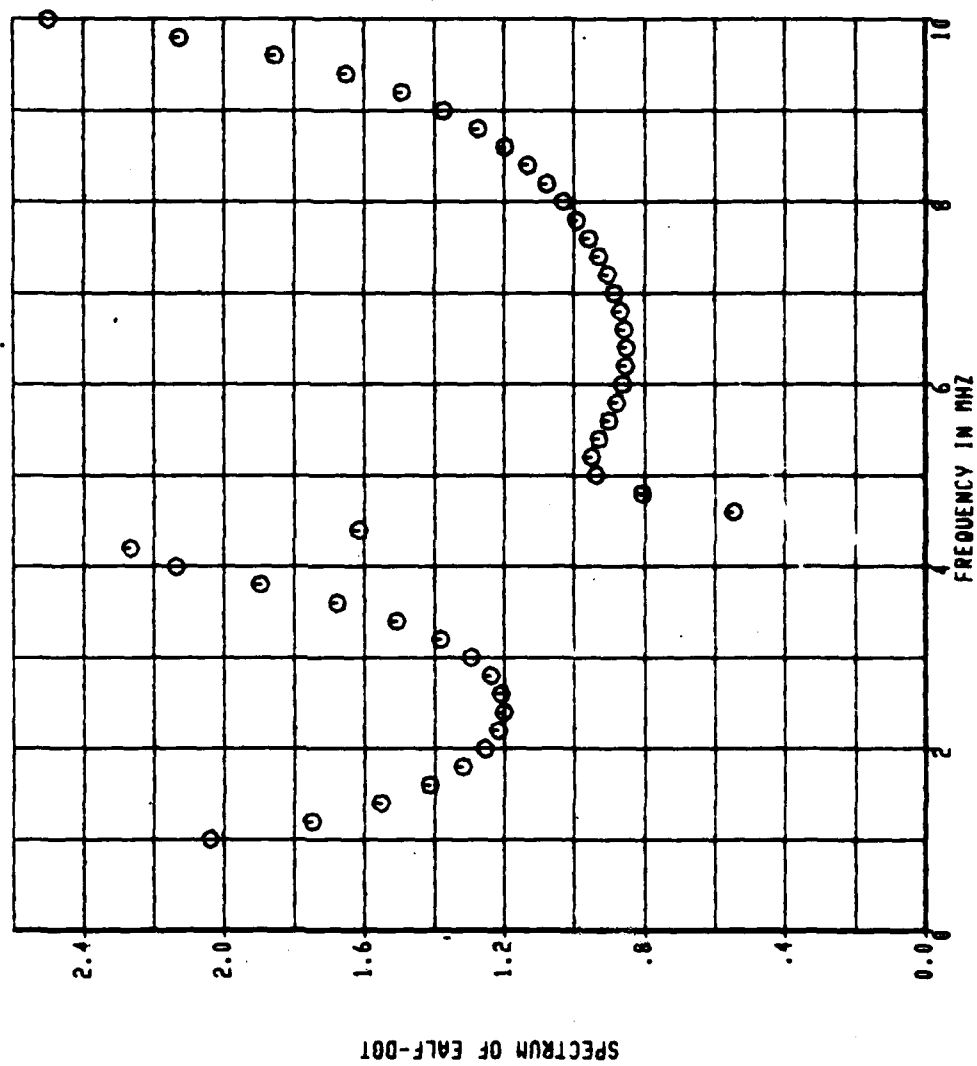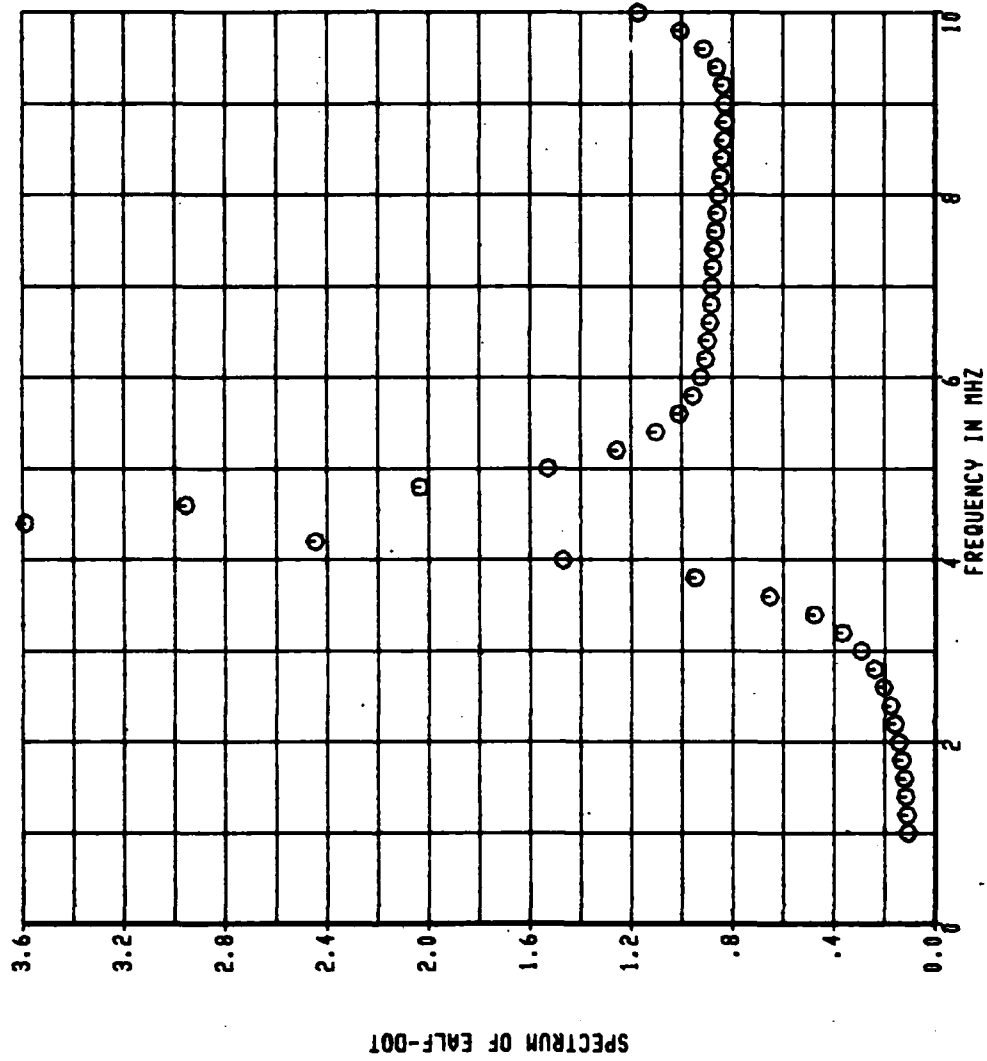
20

ALPHA,THETA,PHI=
0.000000 45.000000 180.000000
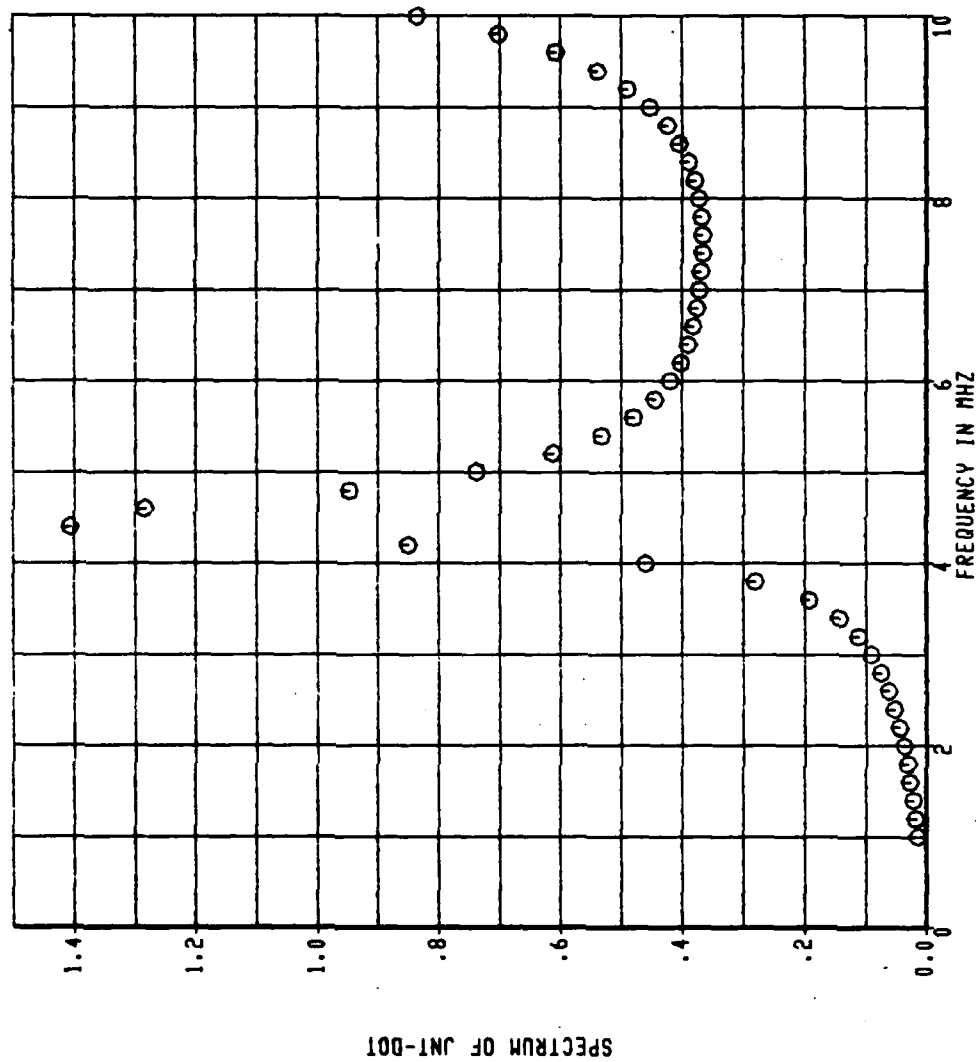
Figure 4C Spectrum of JNT-DOT for incidence along left wing tip obtained from thin-wire model.

21
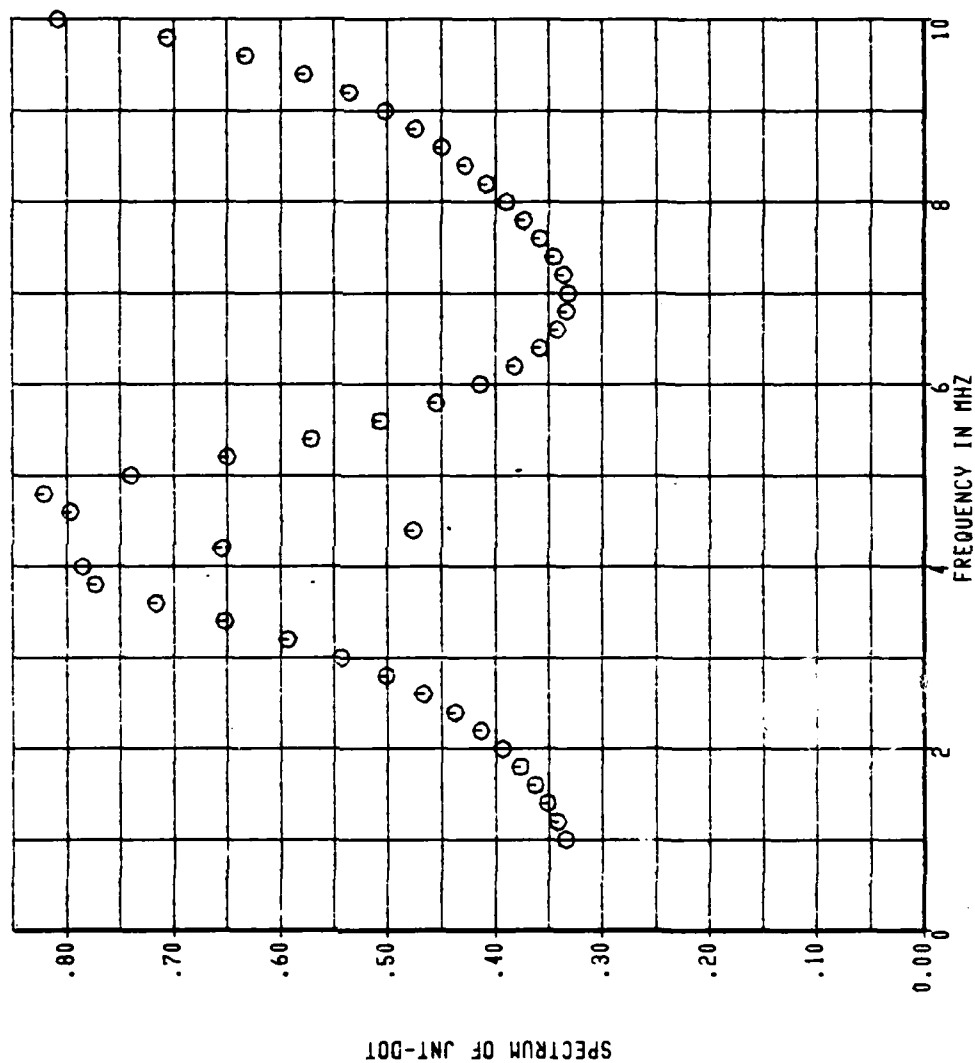
Figure 4D   Spectrum of JNT-DOT for incidence along tail obtained from thin-wire model.

22
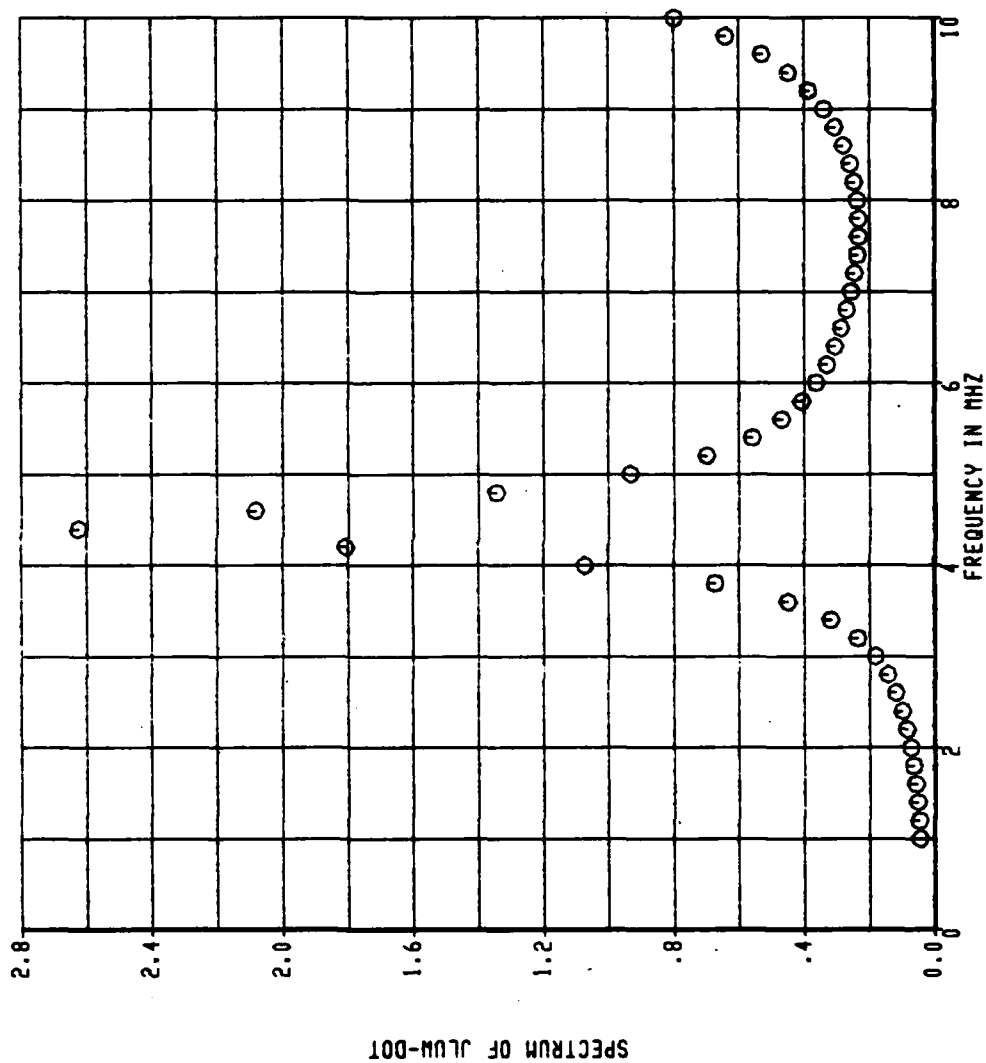
Figure 5A   Spectrum of JLUW-DOT for incidence along nose obtained from thin-wire model.
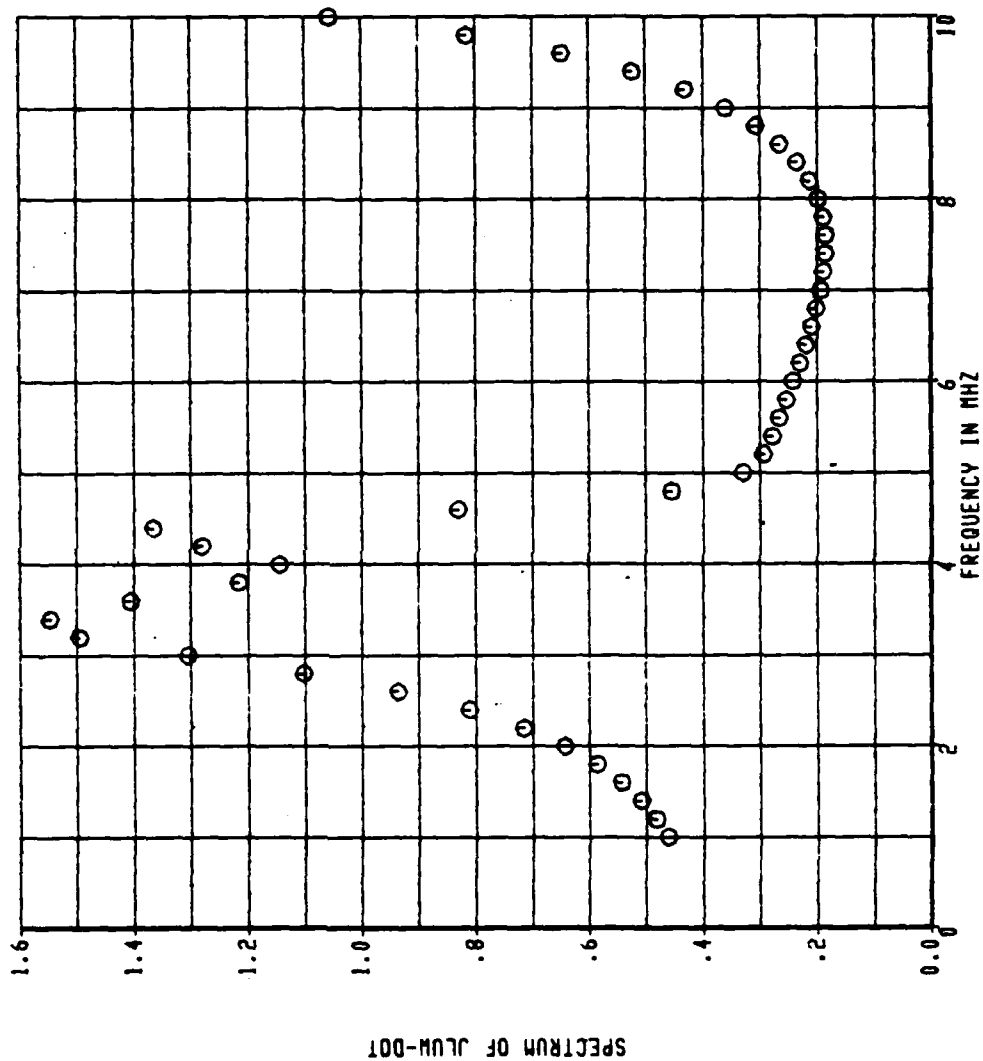
Figure 5B   Spectrum of JLUW-DOT for incidence at 45° to fuselage obtained from thin-wire model.

24
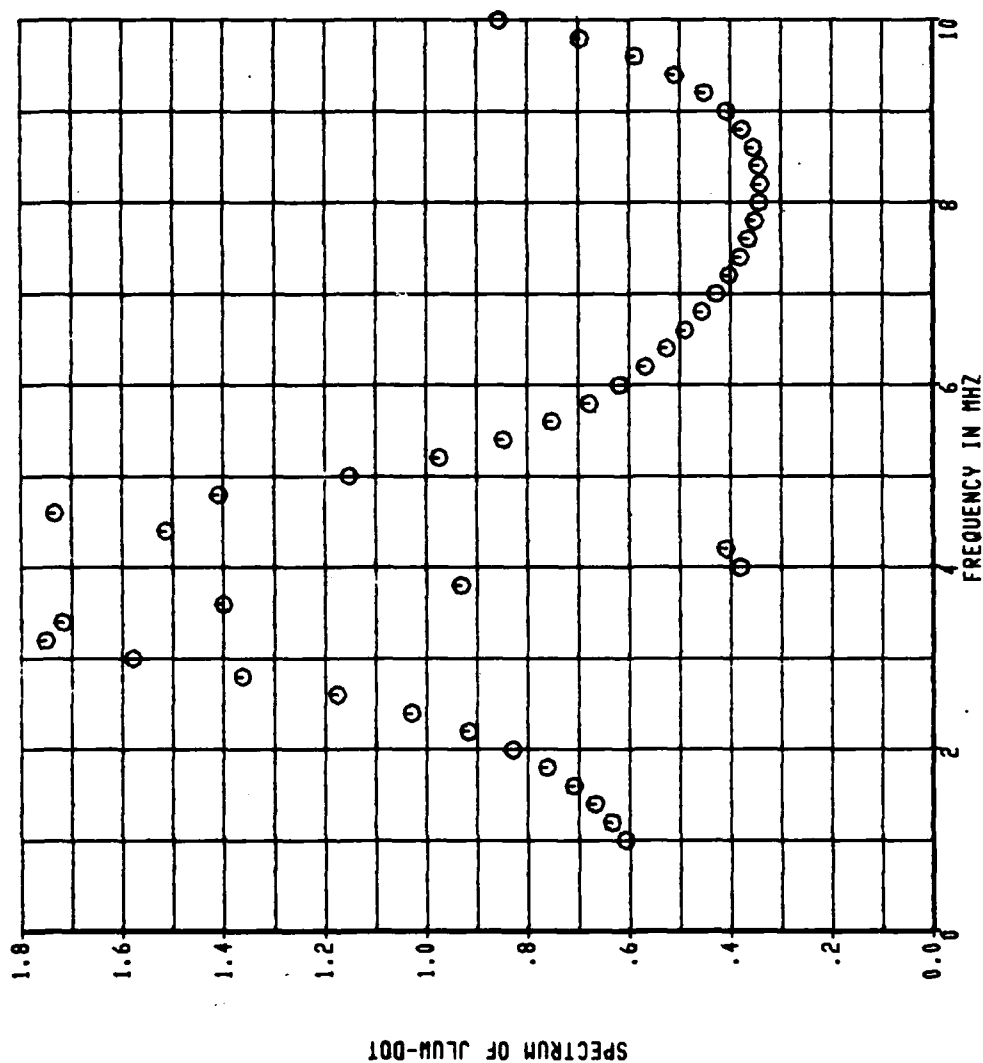
Figure 5C   Spectrum of JLUW-DOT for incidence along left wing tip obtained from thin-wire model.
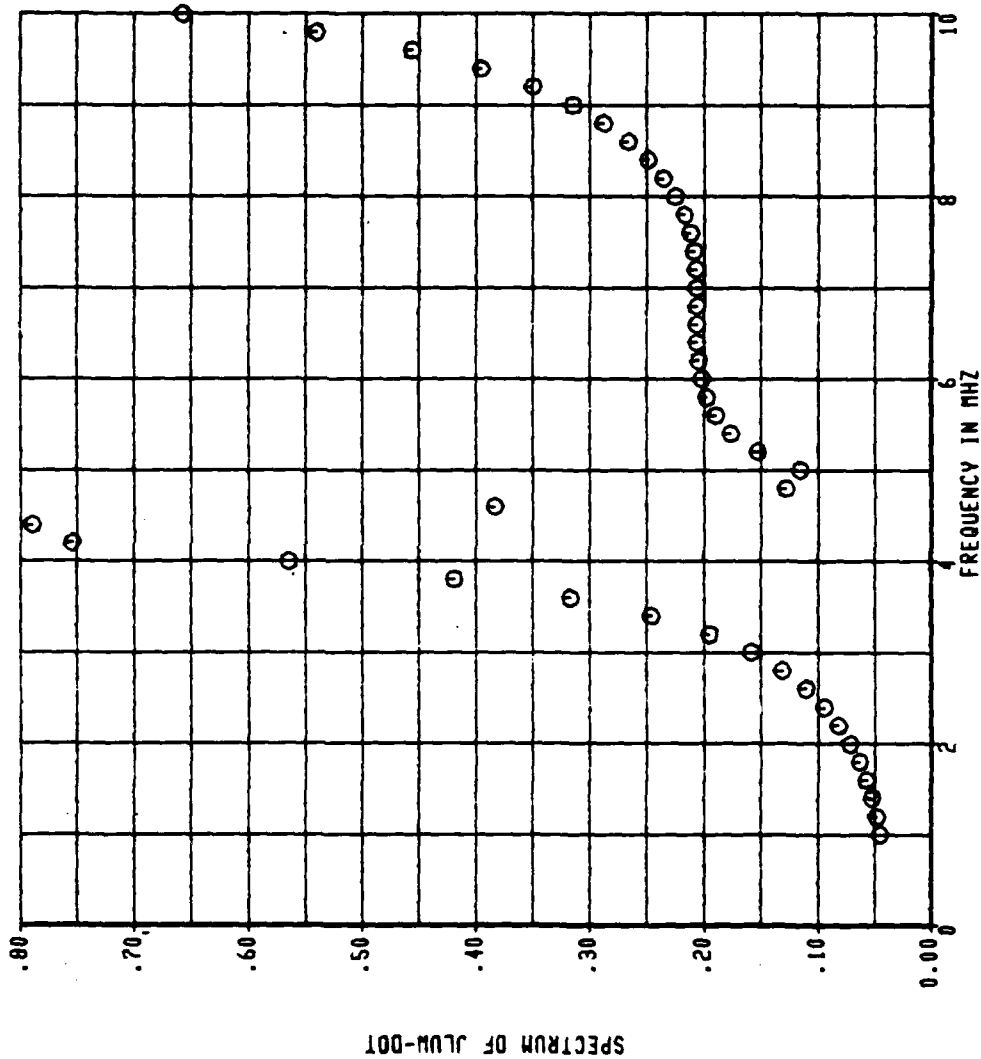
Figure 5D   Spectrum of JLUW-DOT for incidence along tail obtained from thin-wire model.

26

Figure 6A   Spectrum of EALF-DOT for incidence along nose obtained from thin-wire model.

Figure 6B   Spectrum of EALF-DOT for incidence at 45° to fuselage obtained from thin-wire model.

Figure 6C   Spectrum of EALF-DOT for incidence along left wing tip obtained from thin-wire model.
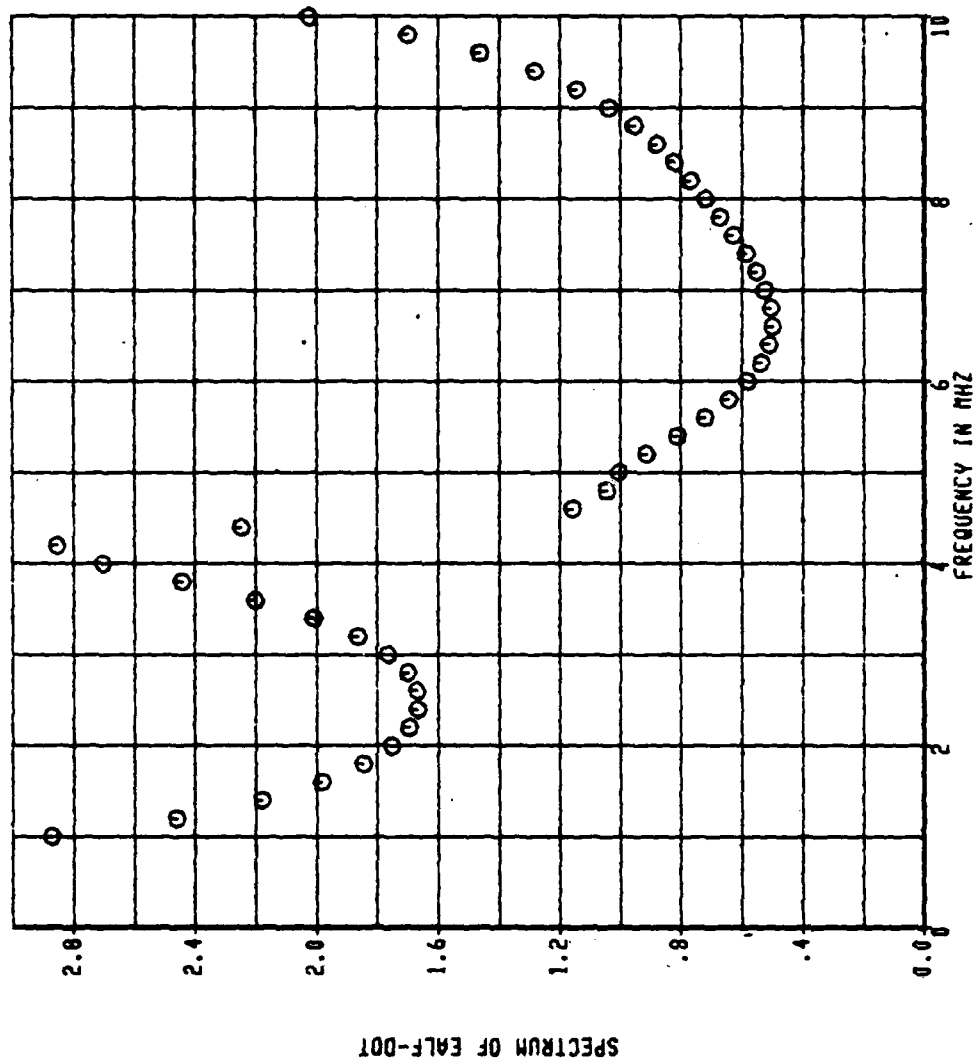
Figure 60   Spectrum of EALF-FOT for incidence along tail obtained from thin-wire model.
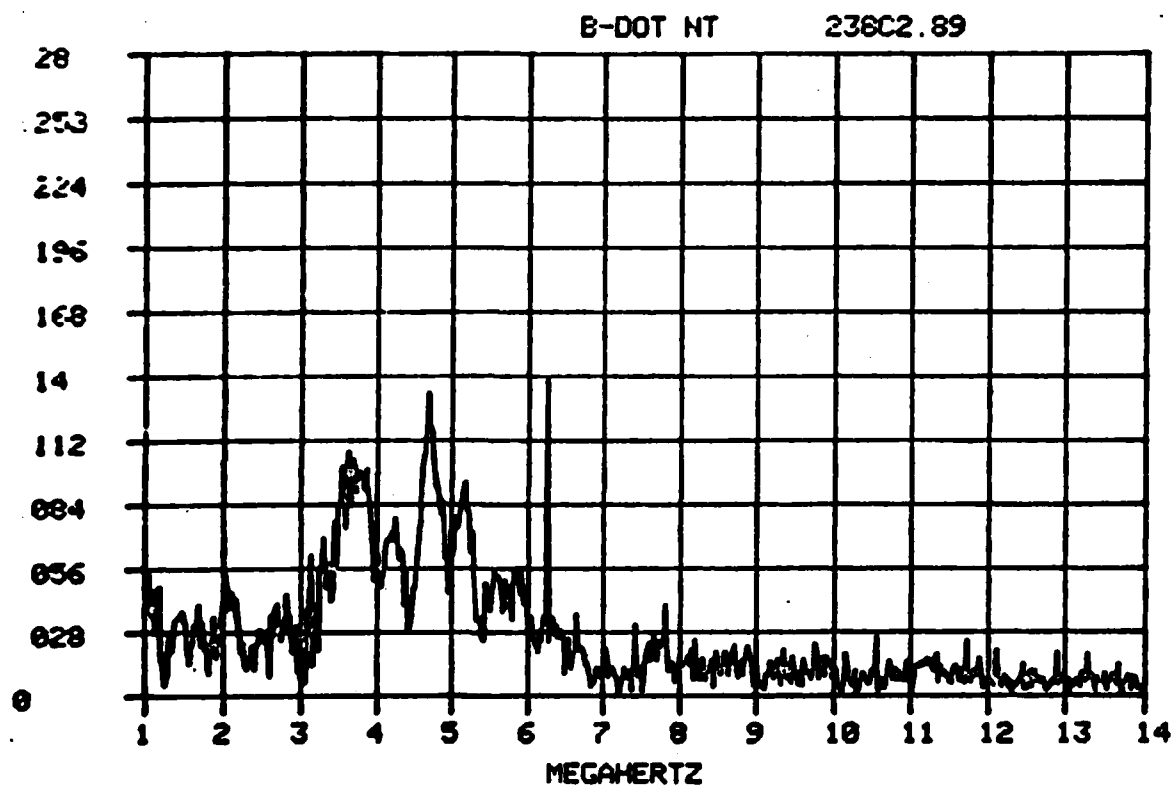
Figure 7A   Measured data for JNT-DOT spectrum.
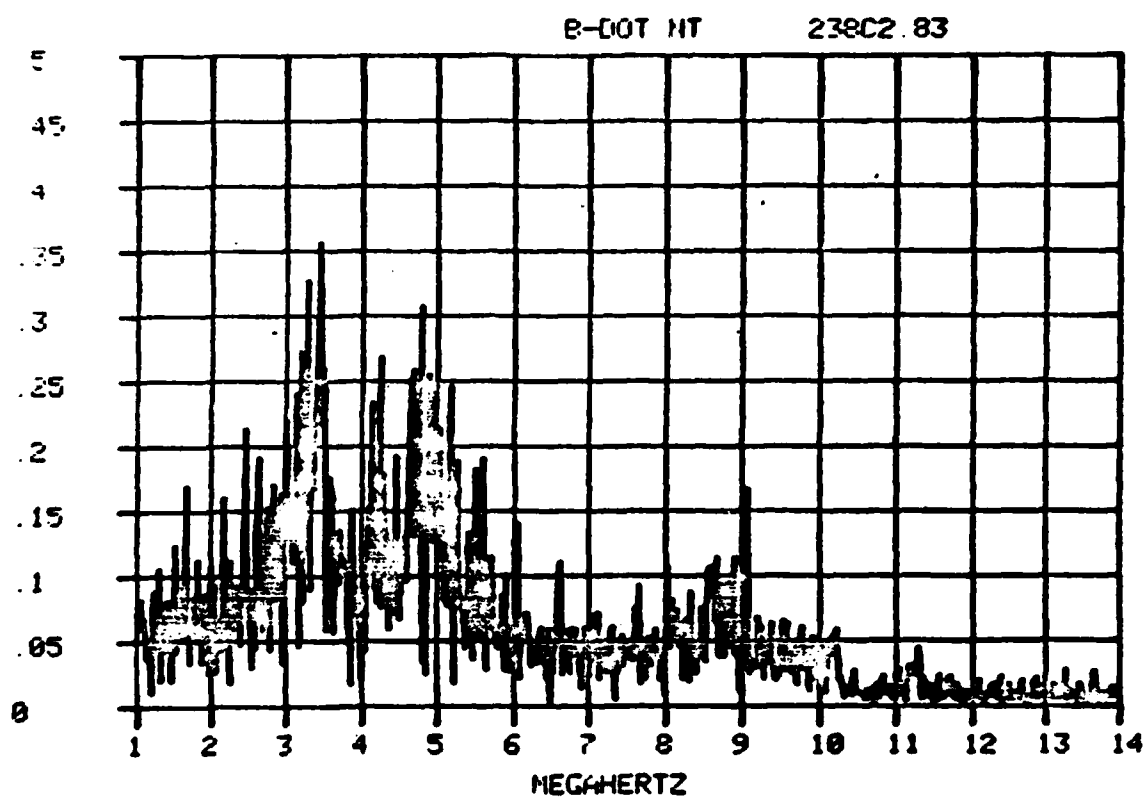
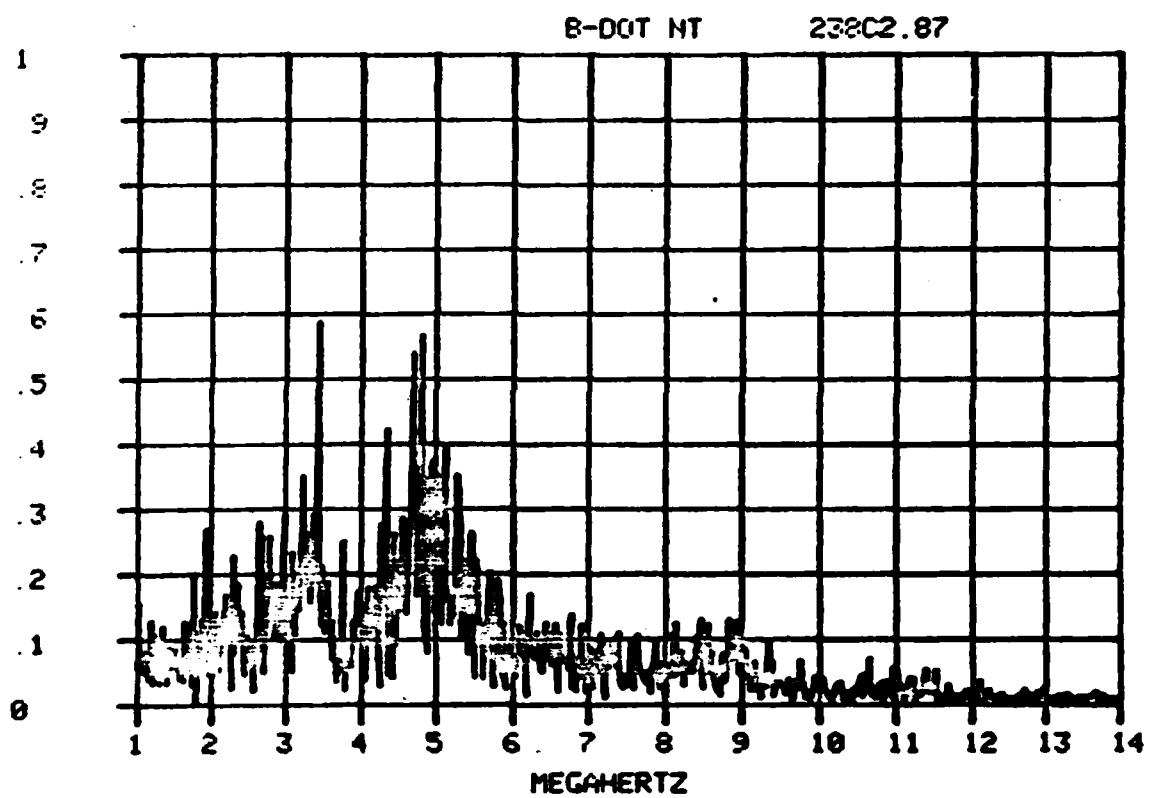Figure 7B   Measured data for JNT-DOT spectrum.

32

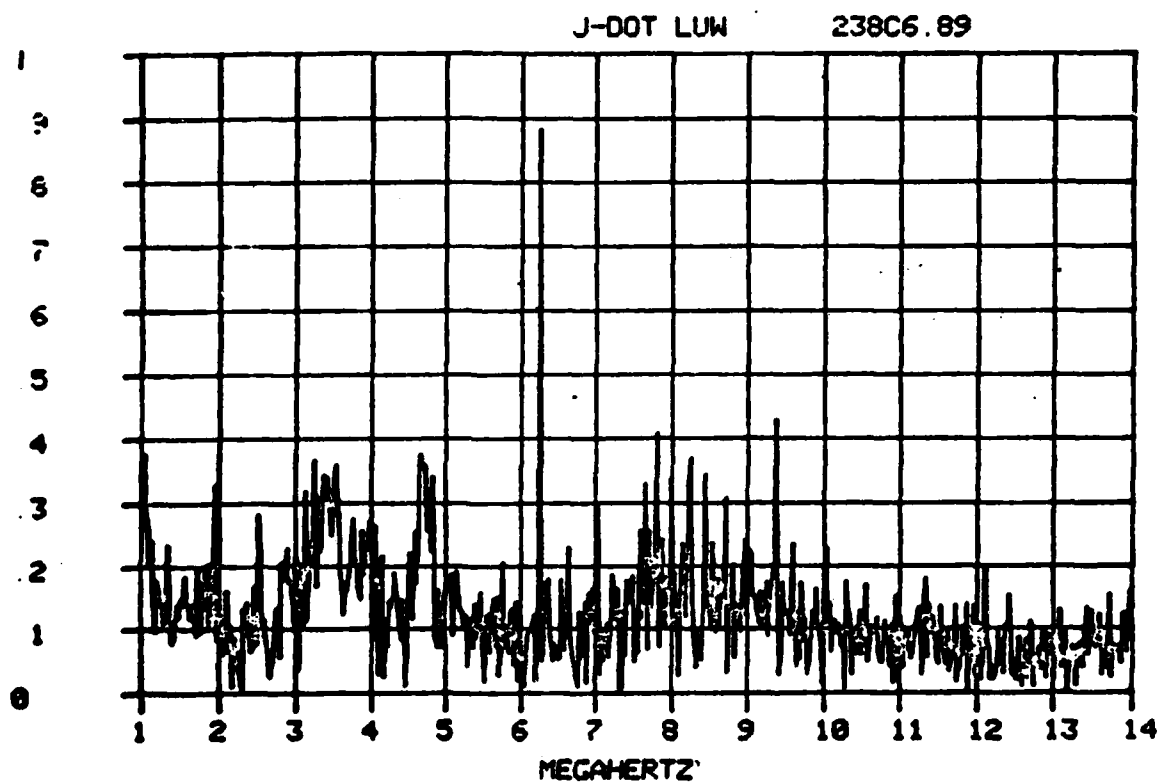Figure 7C   Measured data for JNT-DOT spectrum.

33

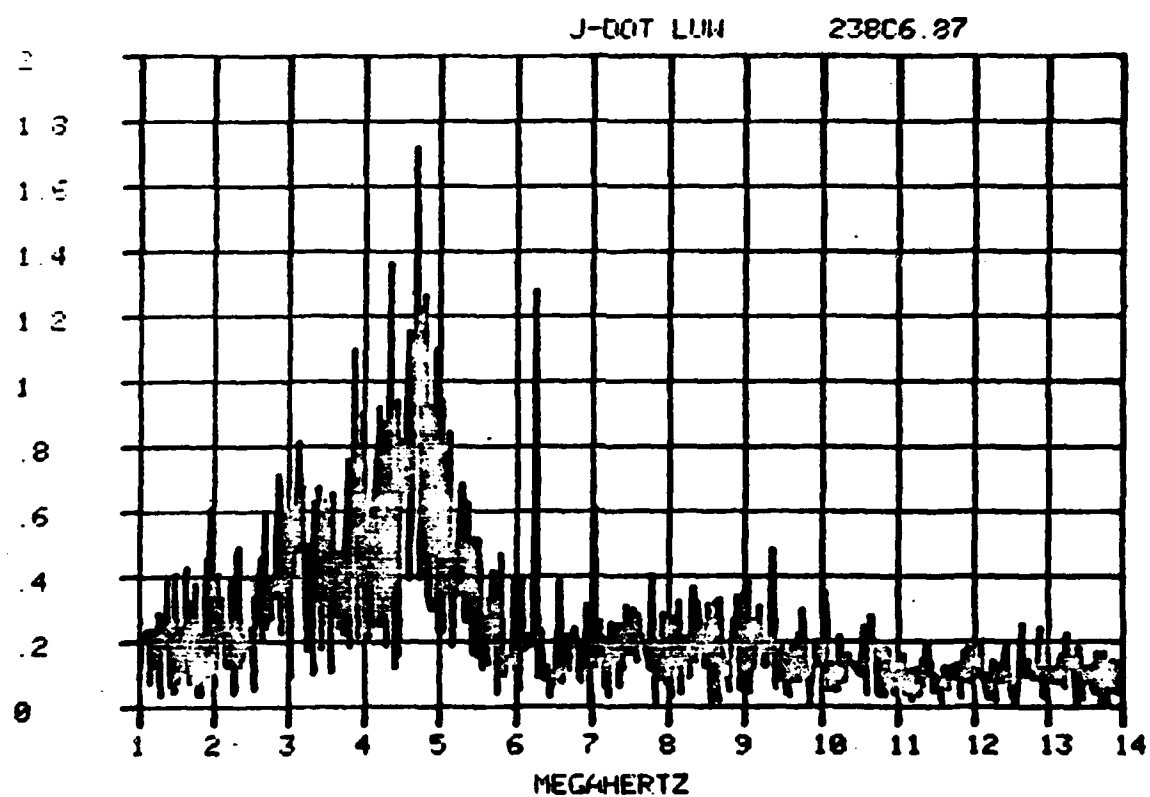Figure 8A   Measured data for JLUW-DOT spectrum.

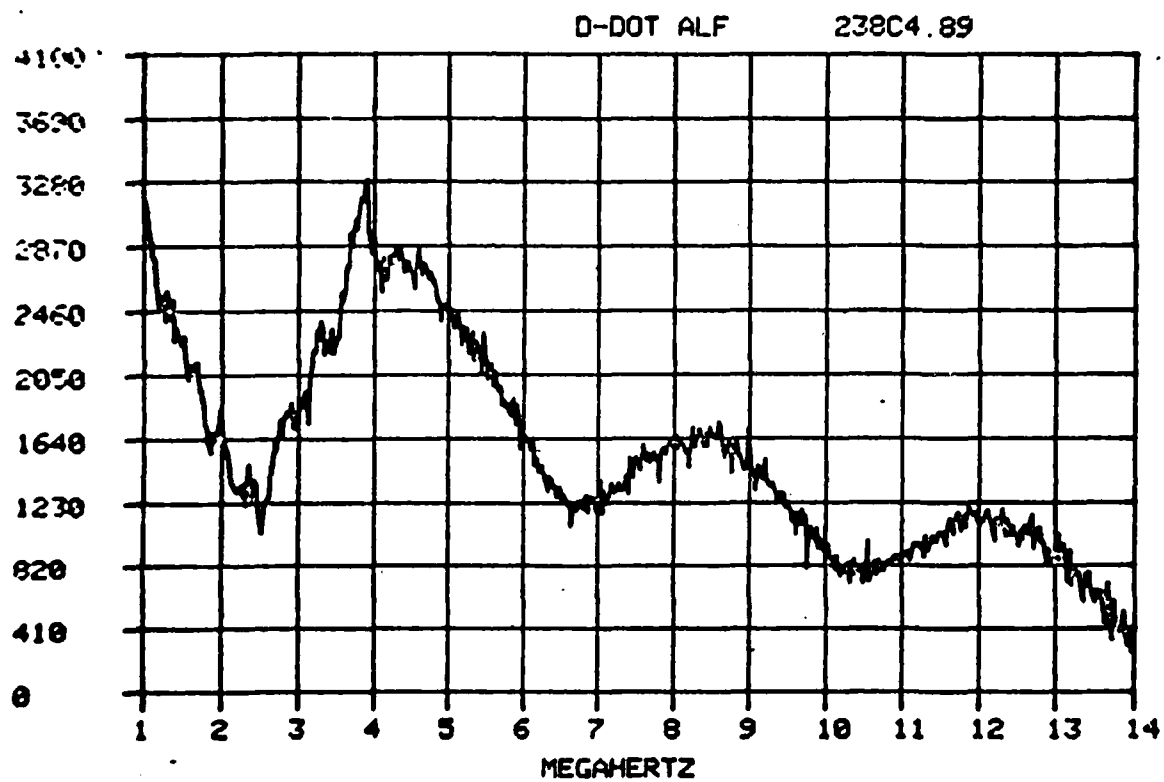Figure 8B   Measured data for JLUW-DOT spectrum.

35

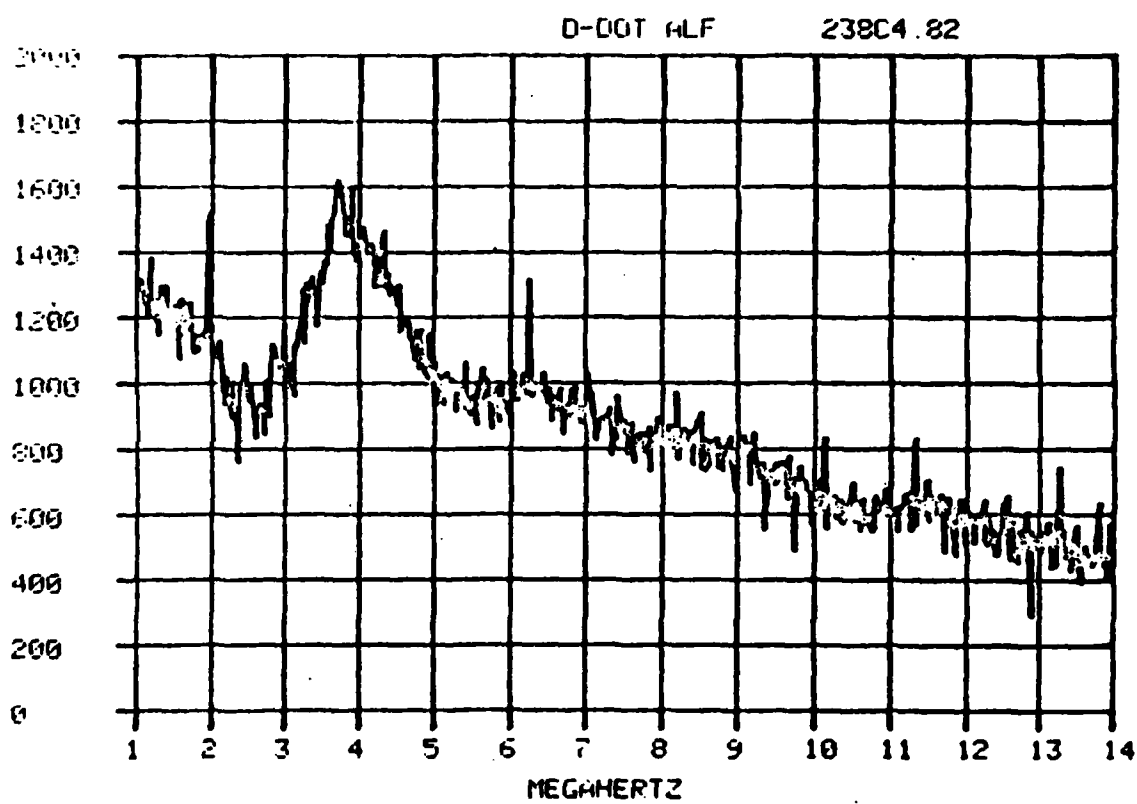Figure 9A   Measured data for EALF-DOT spectrum.
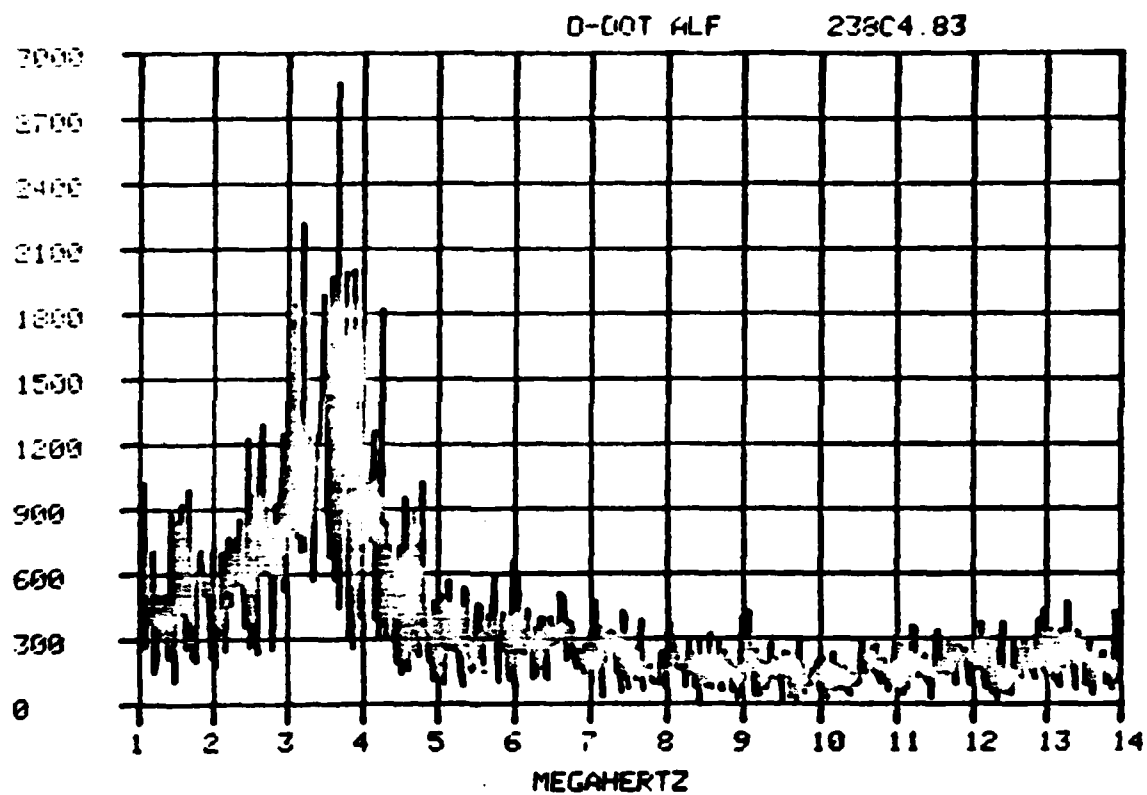
36

Figure 9B   Measured data for EALF-DOT spectrum.

Figure 9C   Measured data for EALF-DOT spectrum.

SECTION VI
RECOMMENDATIONS FOR DATA REDUCTION

The ultimate objective of this program is to provide to AFWAL/FIESL quantitative procedures for removing airframe effects from the data. Since the sensors are sufficiently broad-band, they only add a multiplicative factor to the overall transfer function. As described in the text, the airframe effects are analytically described by the following:

a. A thin wire model which calculates airframe resonances, together with effective circumference to obtain surface fields.

b. Frequency-independent cylinder and strip models which calculate azimuthal currents and azimuthally-dependent fields.

Although airframe resonances are apparent in the data, their amplitude is often quite small compared to the dominant low frequency response. Figure 10 is a typical integrated waveform for the surface current density (not time derivative) at JLUW. For such a waveform, the peak incident field amplitude may be well approximated by drawing a line through the center of the resonance and using the equations of Table II. The rate-of-rise, however, is more strongly influenced by the resonance. In order to remove resonance effects from rate-of-rise, the following general procedure may be used:

1. Determine the frequency, amplitude, and Q of the resonance from the Fourier transform, and check against the original waveform. This requires having absolute values for the Fourier spectrum. The resonant waveform is a damped sinusoid with undetermined phase.

2. Determine by inspection of the waveform the appropriate relative phase of the resonant waveform. In Figure 10, for example, the resonance is evidently in phase with the low frequency response.

3. Subtract the resonant waveform from the measured data and calculate the resulting rate-of-rise.
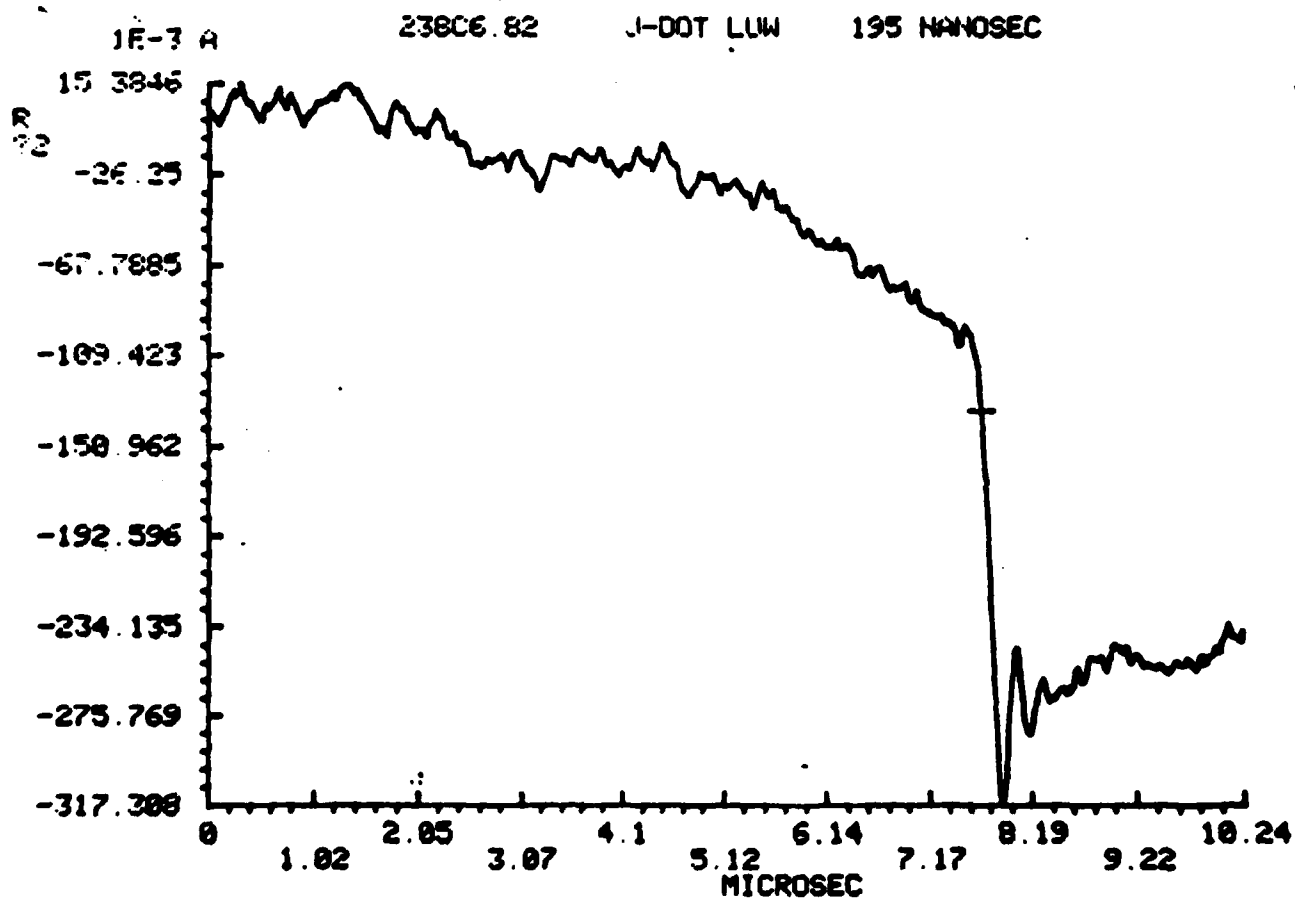
Figure 10   Sample time domain waveform.

This method requires some judgement, particularly in the choice of relative phase. However, for waveforms dominated by a single resonance, it is a good first-order correction to the rate-of-rise data.

The brief discussion of the resonant structure of the measured data points out the following information implicit in the relative amplitudes of the airframe resonances.

1. Orientation of the aircraft relative to the incident plane wave.

2. The high-frequency roll-off of the lightning spectrum.

Along this line, a recommendation for spectral analysis is to limit the time interval to the leading edge of the waveform, and to exclude any precursor pulses. This should remove some of the "hash" from the Fourier transforms.

REFERENCES

1. C. D. Taylor, "External Interaction of the Nuclear EMP with Aircraft and Missiles," IEEE Trans. Electromag. Compat. Vol. EMC-20, pages 64-76, dated February 1978.

2. R. W. P. King, "Currents Induced in a Wire Cross by a Plane Wave Incident at an Angle," IEEE Trans. Antennas Propagat., Vol. AP-25, pages 775-781, dated November 1977.

3. R. W. P. King and B. H. Sandler, "Analysis of Currents Induced in a General Wire Cross by a Plane Wave Incident at an Angle with Arbitrary Polarization," IEEE Trans. Antennas propagat., Vol. AP-29, pages 512-520, dated May 1981.

4. J. J. Bowman, T.B.A. Senior, P.L.E. Uslenghi, "Electromagnetic and Acoustic Scattering by Simple Shapes," John Wiley and Sons, 1969.

5. R. H. West and D. D. Connell, "Antenna Effective Length Measurement," DNA Contract No. DNA 001-75-C-0131, dated July 15, 1975, published by NTIS.

DATE
FILMED

5-8